

Precise measurement of $\Gamma(K_S \rightarrow \pi^+\pi^-(\gamma))/\Gamma(K_S \rightarrow \pi^0\pi^0)$ with the KLOE detector at DAΦNE

The KLOE Collaboration

F. Ambrosino^e, A. Antonelli^b, M. Antonelli^b, C. Bacciⁱ,
 P. Beltrame^c, G. Bencivenni^b, S. Bertolucci^b, C. Bini^g,
 C. Bloise^b, V. Bocci^g, F. Bossi^b, D. Bowring^a, P. Branchiniⁱ,
 R. Caloi^g, P. Campana^b, G. Capon^b, T. Capussela^e,
 F. Ceradiniⁱ, S. Chi^b, G. Chiefari^e, P. Ciambrone^b,
 S. Conetti^a, E. De Lucia^b, A. De Santis^g, P. De Simone^b,
 G. De Zorzi^g, S. Dell'Agnello^b, A. Denig^c, A. Di Domenico^g,
 C. Di Donato^e, S. Di Falco^j, B. Di Miccoⁱ, A. Doria^e,
 M. Dreucci^b, G. Felici^b, A. Ferrari^c, M. L. Ferrer^b,
 G. Finocchiaro^b, S. Fiore^g, C. Forti^b, P. Franzini^g, C. Gatti^{b,1},
 P. Gauzzi^g, S. Giovannella^b, E. Gorini^d, E. Grazianiⁱ,
 M. Incagli^j, W. Kluge^c, V. Kulikov^m, F. Lacava^g,
 G. Lanfranchi^b, J. Lee-Franzini^{b,k}, D. Leone^c, M. Martini^b,
 P. Massarotti^e, W. Mei^b, S. Meola^e, S. Miscetti^b,
 M. Moulson^b, S. Müller^c, F. Murtas^b, M. Napolitano^e,
 F. Nguyenⁱ, M. Palutan^{b,2}, E. Pasqualucci^g, A. Passeriⁱ,
 V. Patera^{b,f}, F. Perfetto^e, L. Pontecorvo^g, M. Primavera^d,
 P. Santangelo^b, E. Santovetti^h, G. Saracino^e, B. Sciascia^b,
 A. Sciubba^{b,f}, F. Scuri^j, I. Sfilogi^b, T. Spadaro^{b,3}, M. Testa^g,
 L. Tortoraⁱ, P. Valente^b, B. Valeriani^c, G. Venanzoni^b,
 S. Veneziano^g, A. Ventura^d, R. Versaci^c, G. Xu^{b,ℓ},

^a*Physics Department, University of Virginia, Charlottesville, VA, USA.*

^b*Laboratori Nazionali di Frascati dell'INFN, Frascati, Italy.*

^c*Institut für Experimentelle Kernphysik, Universität Karlsruhe, Germany.*

^d*Dipartimento di Fisica dell'Università e Sezione INFN, Lecce, Italy.*

^e*Dipartimento di Scienze Fisiche dell'Università "Federico II" e Sezione INFN, Napoli, Italy*

^f*Dipartimento di Energetica dell'Università "La Sapienza", Roma, Italy.*

^g*Dipartimento di Fisica dell'Università “La Sapienza” e Sezione INFN, Roma, Italy.*

^h*Dipartimento di Fisica dell'Università “Tor Vergata” e Sezione INFN, Roma, Italy.*

ⁱ*Dipartimento di Fisica dell'Università “Roma Tre” e Sezione INFN, Roma, Italy.*

^j*Dipartimento di Fisica dell'Università e Sezione INFN, Pisa, Italy.*

^k*Physics Department, State University of New York at Stony Brook, NY, USA.*

^l*Permanent address: Institute of High Energy Physics, CAS, Beijing, China.*

^m*Permanent address: Institute for Theoretical and Experimental Physics, Moscow, Russia.*

¹ Corresponding author: Claudio Gatti INFN - LNF, Casella postale 13, 00044 Frascati (Roma), Italy; tel. +39-06-94032727, e-mail claudio.gatti@lnf.infn.it

² Corresponding author: Matteo Palutan INFN - LNF, Casella postale 13, 00044 Frascati (Roma), Italy; tel. +39-06-94032697, e-mail matteo.palutan@lnf.infn.it

³ Corresponding author: Tommaso Spadaro INFN - LNF, Casella postale 13, 00044 Frascati (Roma), Italy; tel. +39-06-94032698, e-mail tommaso.spadaro@lnf.infn.it

Abstract

Using a sample of over 400 million K_SK_L pairs produced during the years 2001 and 2002 at the DAΦNE e^+e^- collider, the ratio $R_S^\pi = \Gamma(K_S \rightarrow \pi^+\pi^-(\gamma))/\Gamma(K_S \rightarrow \pi^0\pi^0)$ has been measured with the KLOE detector. The result is $R_S^\pi = 2.2555 \pm 0.0012_{\text{stat}} \pm 0.0021_{\text{syst-stat}} \pm 0.0050_{\text{syst}}$, which is in good agreement with the previously published result, based on the KLOE data sample from the year 2000. The average of the KLOE results is $R_S^\pi = 2.2549 \pm 0.0054$, reducing the total error by a factor of three, to 0.25%.

1 Introduction

The ratio $R_S^\pi = \Gamma(K_S \rightarrow \pi^+\pi^-(\gamma))/\Gamma(K_S \rightarrow \pi^0\pi^0)$ is a fundamental parameter of the K_S meson. It provides with almost no corrections the branching ratio (BR) for the two dominant decays of the short lived neutral kaon: $K_S \rightarrow \pi^0\pi^0$ and $K_S \rightarrow \pi^+\pi^-(\gamma)$. The latter BR is a convenient normalization for the BR's of all other K_S decays to charged particles. In particular, it is used to obtain $\Gamma(K_S \rightarrow \pi e \nu)$, which is of interest in testing many predictions of the Standard Model, as discussed in an accompanying paper [1]. From R_S^π one can also derive phenomenological parameters of the kaon system such as the relative magnitude and phase of the $I = 0, 2$ $\pi\pi$ -scattering amplitudes.

Isospin-breaking effects and radiative corrections to the scattering amplitudes are discussed in Refs.2,3. Finally, R_S^π enters into the double ratio that measures direct CP violation in $K \rightarrow \pi\pi$ transitions:

$$R_S^\pi/R_L^\pi = 1 - 6\Re(\epsilon'/\epsilon), \quad (1)$$

where $R_L^\pi = \Gamma(K_L \rightarrow \pi^+\pi^-(\gamma))/\Gamma(K_L \rightarrow \pi^0\pi^0)$. The most accurate measurement of R_S^π was performed by KLOE using data collected in 2000 for an integrated luminosity of $\mathcal{L} \sim 17 \text{ pb}^{-1}$: $R_S^\pi = 2.236 \pm 0.003_{\text{stat}} \pm 0.015_{\text{syst}}$ [4]. This result, more precise than the PDG average of the time [5], for the first time properly included photon radiation and increased the value for $\text{BR}(K_S \rightarrow \pi^+\pi^-(\gamma))$ by 0.5% [6]. The overall accuracy of the previous result, 0.7%, was limited by systematic uncertainties. The present result is based on the analysis of 410 pb^{-1} of integrated luminosity acquired during the years 2001 and 2002, and improves on the total error by a factor of three, to 0.25%.

2 Experimental setup

The data were collected with the KLOE detector at DAΦNE, the Frascati ϕ -factory. DAΦNE is an e^+e^- collider which operates at a center of mass energy of $\sim 1020 \text{ MeV}$, the mass of the ϕ meson. Positron and electron beams of equal energy collide at an angle of $\pi - 25 \text{ mrad}$, producing ϕ mesons with a small momentum in the horizontal plane: $p(\phi) \sim 13 \text{ MeV}/c$. ϕ mesons decay $\sim 34\%$ of the time into nearly collinear $K^0\bar{K}^0$ pairs. Because $J^{PC}(\phi) = 1^{--}$, the kaon pair is in an antisymmetric state, so that the final state is always K_SK_L . The contamination from $K_L K_L \gamma$ and $K_S K_S \gamma$ final states is negligible for this measurement [7, 8]. Therefore, the detection of a K_L signals the presence of a K_S of known momentum and direction, independently of its decay mode. This technique is called K_S *tagging* in the following. A total of ~ 1.3 billion ϕ mesons were produced, yielding ~ 430 million K_SK_L pairs.

The KLOE detector consists of a large cylindrical drift chamber (DC) surrounded by a lead scintillating-fiber sampling calorimeter (EMC). A superconducting coil surrounding the calorimeter provides a 0.52 T magnetic field. The drift chamber [9], which is 4 m in diameter and 3.3 m long, has 12582 all-stereo tungsten sense wires and 37746 aluminum field wires. The chamber shell is made of carbon-fiber epoxy composite and the gas used is a 90% helium, 10% isobutane mixture. These features maximize transparency to photons and reduce $K_L \rightarrow K_S$ regeneration and multiple scattering. The position resolutions are $\sigma_{xy} \approx 150 \mu\text{m}$ and $\sigma_z \approx 2 \text{ mm}$. The momentum resolution is $\sigma(p_\perp)/p_\perp \approx 0.4\%$. Vertices are reconstructed with a spatial resolution of $\approx 3 \text{ mm}$.

The calorimeter [10] is divided into a barrel and two endcaps, contains a total of 88 modules, and covers 98% of the solid angle. The modules are read out at both ends by photomultiplier tubes. The arrival times of particles and the three-dimensional positions of the energy deposits are determined from the signals at the two ends. The readout granularity is $\sim 4.4 \times 4.4 \text{ cm}^2$; the 2440 “cells” are arranged in layers five-deep. Cells close in time and space are grouped into a “calorimeter cluster.” For each cluster, the energy E_{cl} is the sum of the cell energies, and the time t_{cl} and position \vec{r}_{cl} are calculated as energy-weighted averages over the fired cells. The energy and time resolutions are $\sigma_E/E = 5.7\%/\sqrt{E(\text{GeV})}$ and $\sigma_t = 57 \text{ ps}/\sqrt{E(\text{GeV})} \oplus 100 \text{ ps}$, respectively.

While the trigger [11] uses calorimeter and chamber information, only the calorimeter trigger, which requires two local energy deposits above threshold (50 MeV in the barrel or 150 MeV in the endcaps), is used for the present measurement. Recognition and rejection of cosmic-ray events is also performed at the trigger level: events with two energy deposits above a 30 MeV threshold in the outermost calorimeter plane are rejected as cosmic-ray events. To reject residual cosmic rays and machine background events an offline software filter (FIFO) has been designed, which exploits calorimeter information before tracks are reconstructed.

The trigger has a large time spread with respect to the beam crossing time. However, it is synchronized with the machine RF divided by 4, $T_{\text{sync}} \sim 10.8 \text{ ns}$, with an accuracy of 50 ps. The time of the bunch crossing producing an event is determined offline during event reconstruction.

The response of the detector to the decays of interest and the various backgrounds were studied by using the Monte Carlo (MC) simulation program [12]. The MC accounts for changes in the machine operation and background conditions in order to reproduce real data on a run-by-run basis. The most important parameters are the beam energies and crossing angle, obtained from the analysis of Bhabha scattering events, and the rate of accidental clusters from the machine (R_{acc}), extracted from the analysis of $e^+e^- \rightarrow \gamma\gamma$ events. R_{acc} is particularly relevant because it significantly affects the acceptance for $\pi^+\pi^-$ and $\pi^0\pi^0$ events, as discussed in the following sections. For the present analysis, an MC sample of $\phi \rightarrow K_SK_L$ decays is used that corresponds to an integrated luminosity of $\sim 550 \text{ pb}^{-1}$; an equivalent integrated luminosity of $\sim 90 \text{ pb}^{-1}$ has been simulated for the other ϕ -meson final states.

3 Signal selection

The decay lengths of the K_S and K_L are $\lambda_S \sim 0.6 \text{ cm}$ and $\lambda_L \sim 350 \text{ cm}$, respectively. About 50% of K_L ’s therefore reach the calorimeter before decaying.

The K_L interaction in the calorimeter barrel (K_L *crash*, K_{cr} in the following) is identified by requiring a cluster of energy above a given threshold not associated with any track, and whose time corresponds to a velocity $\beta = r_{\text{cl}}/c t_{\text{cl}}$ compatible with that of the K_L , $\beta(K_L) \sim 0.216$. A cut is applied on β^* , the K_L velocity transformed to the ϕ rest frame: $0.17 \leq \beta^* \leq 0.28$. These K_{cr} events are used for K_S tagging.

The interaction time, which must be known for the measurement of the cluster times, is obtained from the first particle reaching the calorimeter (pions or photons for the events of interest) assuming a velocity $\beta = 1$. This definition of interaction time (T_0 in the following) does not require the K_S decay to be identified. In order to reduce the probability that T_0 is accidentally determined from a particle due to machine background, the T_0 is required to be given by a cluster with energy $E_{\text{cl}} > 50$ MeV and distance to the beam line $\rho_{\text{cl}} > 60$ cm (T_0 cluster).

$K_S \rightarrow \pi^+ \pi^- (\gamma)$ events are selected by requiring the presence of two tracks of opposite charge with their point of closest approach to the origin inside a cylinder 4 cm in radius and 10 cm in length along the beam line. Pion momenta and polar angles must satisfy the fiducial cuts $120 \leq p \leq 300$ MeV/ c and $30^\circ \leq \theta \leq 150^\circ$. Pions must also reach the EMC, and at least one of them must have an associated T_0 cluster.

$K_S \rightarrow \pi^0 \pi^0$ events are identified by the prompt photon clusters from π^0 decays. A prompt photon cluster must satisfy $|t_{\text{cl}} - r_{\text{cl}}/c| \leq 5\sigma_t$, σ_t being the energy-dependent time resolution, and must not be associated to any track. Machine background is reduced by cuts on cluster energy and polar angle: $E_{\text{cl}} > 20$ MeV and $|\cos \theta| < 0.9$. To accept a $K_S \rightarrow \pi^0 \pi^0$ event, three or more prompt photons are required.

The number N of $\pi^+ \pi^-$ and $\pi^0 \pi^0$ events and the corresponding selection efficiencies ϵ_{sel} are then used to compute R_S^π according to the following equation:

$$R_S^\pi = \frac{\Gamma(K_S \rightarrow \pi^+ \pi^- (\gamma))}{\Gamma(K_S \rightarrow \pi^0 \pi^0)} = \frac{N(\pi^+ \pi^-)}{N(\pi^0 \pi^0)} \frac{\epsilon_{\text{sel}}(\pi^0 \pi^0)}{\epsilon_{\text{sel}}(\pi^+ \pi^-)} \frac{C(\pi^+ \pi^-)}{C(\pi^0 \pi^0)}, \quad (2)$$

where C is the purity of the sample (signal over signal plus background), as evaluated from MC.

4 Efficiency evaluation

The fractional statistical error from the counting is $\sim 0.5 \times 10^{-3}$; the overall uncertainty is dominated by systematics. Therefore, in the analysis great ef-

fort has been put into carefully estimating all possible systematic effects, as discussed in detail in Ref. 13.

The selection efficiency is parametrized for each of the two channels ($\pi^+\pi^-$, $\pi^0\pi^0$) as follows:

$$\epsilon_{\text{sel}} = \epsilon_{\text{tag}} \epsilon_{\text{acc}} \epsilon_{\text{trg}} \epsilon_{\text{CV}} \epsilon_{\text{FILFO}}, \quad (3)$$

where ϵ_{tag} and ϵ_{acc} are the tagging efficiency and the signal acceptance; ϵ_{trg} , ϵ_{CV} , and ϵ_{FILFO} are the efficiencies for the trigger, the cosmic-ray veto, and the offline background filter (FILFO).

The tagging efficiency and acceptance are correlated by the T_0 determination. For essentially all of $K_S \rightarrow \pi^0\pi^0$ selected events, the T_0 corresponds to the true collision time and for the purposes of K_{cr} selection, the velocity β^* is correct (empty histogram of Fig. 1). Events selected by the K_{cr} algorithm given the true value of the collision time are called $K_{\text{cr}}^{\text{true}}$. In contrast, for most of $K_S \rightarrow \pi^+\pi^-$ events the T_0 does not correspond to the true collision time. Indeed, charged pions arrive at the EMC ~ 3 ns later than γ 's from π^0 decays and the time T_0 is therefore delayed by one RF period, $T_{\text{RF}} \sim 2.7$ ns; in a few percent of the cases, larger displacements are observed. This results in a $\sim 10\%$ overestimation of the K_L velocity and a difference in the tail populations (gray histogram of Fig. 1). The net effect on the tagging efficiency of $K_S \rightarrow \pi^+\pi^-$ events is that a fraction $(1 - A) \sim 3\%$ of $K_{\text{cr}}^{\text{true}}$ -events is lost, while a fraction $B \sim 0.3\%$ of non- $K_{\text{cr}}^{\text{true}}$ events creeps into the selection (the fractions A and B are defined more precisely in Sec. 4.1).

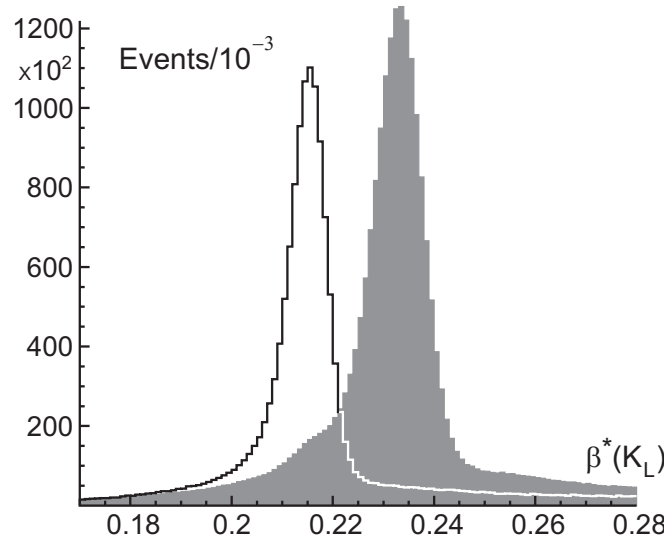


Fig. 1. K_L velocity transformed to the ϕ rest frame, β^* , for $K_S \rightarrow \pi^0\pi^0$ (empty histogram) and $K_S \rightarrow \pi^+\pi^-$ (gray histogram).

Furthermore, $K_{\text{cr}}^{\text{true}}$ and non- $K_{\text{cr}}^{\text{true}}$ events have different topologies: the first

category is dominated by real K_L interactions in the EMC, with β^* laying around the peak; the second category is mostly due to in-flight K_L decays before the EMC. Due to disturbance between K_L and K_S decay products, which undermines reconstruction performance, the signal acceptance $a_{\bar{cr}}$ for the second category is a few percent lower than that for the first category a_{cr} .

The selection efficiency of Eq. 3 is finally expressed combining the acceptances with the probabilities ϵ_{cr} and $1 - \epsilon_{cr}$ for having a K_{cr}^{true} or non- K_{cr}^{true} event, respectively:

$$\epsilon_{\text{sel}} = [\epsilon_{cr} a_{cr} A + (1 - \epsilon_{cr}) a_{\bar{cr}} B] \epsilon_{\text{trg}} \epsilon_{\text{CV}} \epsilon_{\text{FILFO}} \quad (4)$$

The fractions A and B are evaluated using data control samples, while the efficiency ϵ_{cr} is taken from MC (Sec. 4.1). The acceptances a_{cr} and $a_{\bar{cr}}$ are evaluated using MC, with data-driven corrections as explained in Secs. 4.2 and 4.3 for $\pi^+\pi^-$ and $\pi^0\pi^0$ events, respectively. The efficiencies ϵ_{trg} , ϵ_{CV} , and ϵ_{FILFO} are evaluated using data control samples as discussed in Sec. 4.4. All of the efficiencies in Eq. 4 have to be understood as conditional probabilities with respect to the previous step in the analysis, according to the order in which they appear.

The analysis is carried out for three different cuts on the K_L cluster energy: $E_{\text{cr}} = 125$, 200, and 300 MeV. The tagging efficiencies are very different in each case: $\epsilon_{cr} \sim 0.34$, 0.22, and 0.12, respectively. Moreover, some of the corrections applied and the related systematic uncertainties vary considerably with the cut value, thus allowing a test on the robustness of the result.

The data were divided into 17 different samples following variations in the machine energy. The large number of events allowed us to get a statistical error at the per-mil level for each single data period. Comparing the independent measurements from each data sample provides a stringent stability test. The final result is obtained by averaging the results from each sample, while numerical details concerning all of the quantities involved in Eqs. 2 and 4 are given in the following sections for a representative sample (no. 10).

4.1 Tagging efficiencies

This section concerns the evaluation of the quantities involved in the tagging efficiency: A , B , and ϵ_{cr} .

The following parametrizations are used: $A = \sum_n f_n P_n^{\text{in}}$, $B = \sum_n f_n P_n^{\text{out}}$, where

- f_n is the T_0 spectrum, *i.e.*, the fraction of events in which T_0 is shifted by $n \times T_{\text{RF}}$ with respect to the true collision time T_0^{true} ;

- P_n^{in} is the probability that, given a $K_{\text{cr}}^{\text{true}}$ found, the K_{cr} tag is again found even after the T_0 determination is shifted by $n \times T_{\text{RF}}$;
- P_n^{out} is the probability that, without a $K_{\text{cr}}^{\text{true}}$ found, a K_{cr} tag is newly found after the T_0 determination is shifted by $n \times T_{\text{RF}}$.

All of these quantities are taken from data control samples.

The T_0 spectrum (f_n) is evaluated for both $\pi^+\pi^-$ and $\pi^0\pi^0$ events after the signal selection requests have been applied. For the charged mode, a subsample of $K_S \rightarrow \pi^+\pi^-$ events is selected in which both charged pions are associated to clusters. For each pion, an estimate of T_0^{true} is obtained from the cluster time and the time of flight calculated from the track. The robustness of this estimate is increased by requiring that both pions give the same result. The f_n spectrum is obtained as the normalized distribution of $(T_0 - T_0^{\text{true}})/T_{\text{RF}}$ (Fig. 2). As previously mentioned, T_0 overestimates the true collision time by one RF period $\sim 97\%$ of the time. The negative tail of the spectrum shows peaks corresponding to the bunch-crossing times, and is dominated by events in which T_0 is determined by a cluster from machine background, occurring at random with respect to the collision time. For $\pi^0\pi^0$ events the situation is

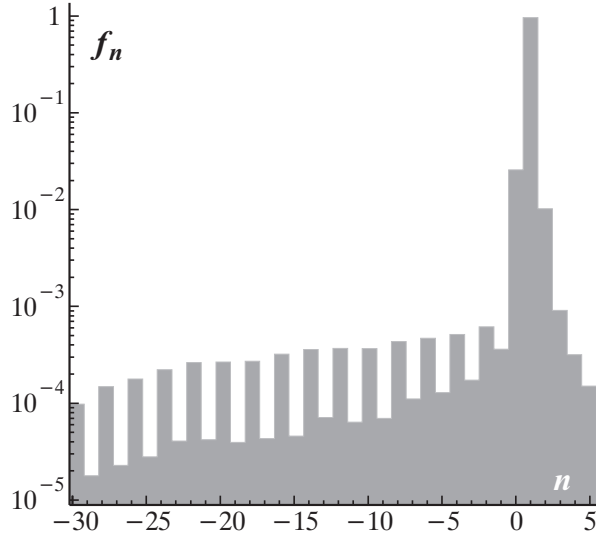


Fig. 2. f_n spectrum for $K_S \rightarrow \pi^+\pi^-$ selected events.

much simpler, because the request of having at least three prompt clusters is fulfilled only if $T_0 = T_0^{\text{true}}$. Therefore f_n is negligible for $n \neq 0$, and the values $A(\pi^0\pi^0) = 1$ and $B(\pi^0\pi^0) = 0$ are used.

For the charged mode, the probabilities P_n^{in} and P_n^{out} are needed for the evaluation of A and B . For this purpose, a sample of events selected on the basis of a reconstructed $K_S \rightarrow \pi^+\pi^-$ decay (without reference to the K_{cr} tag) is used. The estimate of the true collision time T_0^{true} described above is used to divide these events into $K_{\text{cr}}^{\text{true}}$ and non- $K_{\text{cr}}^{\text{true}}$. The T_0 value is then artificially shifted by $n \times T_{\text{RF}}$ with respect to T_0^{true} . For $K_{\text{cr}}^{\text{true}}$ events, the probability P_n^{in}

of still finding the K_{cr} is evaluated, as is the probability P_n^{out} of finding a K_{cr} not originally present for non- $K_{\text{cr}}^{\text{true}}$ events. From the probabilities f_n , P_n^{in} , and P_n^{out} the fractions A and B are calculated. The results for $\pi^+\pi^-$ events are listed in Tab. 1. The value of $A(\pi^+\pi^-)$ increases with E_{cr} , reaching $\sim 99\%$ for $E_{\text{cr}}=300 \text{ MeV}$. The tails of the β^* spectrum are indeed suppressed by increasing the K_{cr} energy cut. This reduces the acceptance losses as a consequence of an incorrect T_0 determination. The maximal variation of $A(\pi^+\pi^-)$ along the data taking is $\sim 1\%$.

Possible biases in the estimate of the f_n spectra have been checked using the MC, by evaluating the ratio A^{true}/A . Here, A^{true} is evaluated from MC truth and A is evaluated with the same method used for data. The difference between results obtained with and without applying the above ratio as a correction to the estimate of A for data is taken as a systematic error; this error is 0.25×10^{-3} for $E_{\text{cr}}=300 \text{ MeV}$. Given the small value of $B(\pi^+\pi^-)$, no correction is applied. A similar comparison with MC truth allows a systematic error of $\sim 0.4 \times 10^{-3}$ to be assigned to the assumption $A(\pi^0\pi^0)=1$. The total systematic error from the evaluation of the f_n spectra and of the probabilities $P_n^{\text{in}}, P_n^{\text{out}}$ is 0.45×10^{-3} at $E_{\text{cr}}=300 \text{ MeV}$ (see Tab. 5).

When computing the ratio between $\pi^+\pi^-$ and $\pi^0\pi^0$ selection efficiencies (see Eqs. 2 and 4) the value of the ratio $\epsilon_{\text{cr}}(\pi^+\pi^-)/\epsilon_{\text{cr}}(\pi^0\pi^0)$ is needed. This ratio varies with E_{cr} , ranging from ~ 1.003 at 125 MeV to ~ 1.01 at 300 MeV (Tab. 1). This is due to the geometrical overlap in the EMC between K_S daughter particles and the K_L , which affects the K_{cr} reconstruction efficiency in a manner dependent on the decay channel. For $\pi^+\pi^-$ events, the efficiency drops when pions get closer to the K_L because of the higher probability of associating the K_L cluster to one pion track; for $\pi^0\pi^0$ events, a drop is observed when a K_S photon and the K_L hit the same calorimeter cell, thus spoiling the cluster reconstruction. These biases are not present when K_S -daughter particles enter the EMC far away from the point of impact of the K_L . The MC evaluation of $\epsilon_{\text{cr}}(\pi^+\pi^-)/\epsilon_{\text{cr}}(\pi^0\pi^0)$ is corrected to account for data-MC differences with a systematic error of $\sim 0.44 \times 10^{-3}$ for $E_{\text{cr}}=300 \text{ MeV}$ (Tab. 5).

E _{cr} cut		125 MeV	200 MeV	300 MeV
$\pi^+\pi^-$	A	0.9634(1)	0.9866(1)	0.9933(1)
	$B(\times 10^{-3})$	3.4489(6)	1.6675(1)	0.71563(3)
	ϵ_{cr}	0.3106(2)	0.2231(2)	0.1082(2)
$\pi^0\pi^0$	ϵ_{cr}	0.3097(3)	0.2217(3)	0.1067(2)

Table 1

Tagging probabilities which enter in the evaluation of the selection efficiency (Eq. 4) for $\pi^+\pi^-$ and $\pi^0\pi^0$ events, for data sample no. 10 and minimum K_{cr} energies of 125, 200, and 300 MeV. Statistical errors are shown in parentheses.

4.2 Acceptance and purity for $K_S \rightarrow \pi^+\pi^-(\gamma)$

The $\pi^+\pi^-$ acceptance is evaluated from MC. Since no cut is applied on the $\pi\pi$ invariant mass, the selection includes $K_S \rightarrow \pi^+\pi^-\gamma$ events with photon energies up to the end point (~ 160 MeV in the K_S rest frame). However, due to the requirement of having both pions extrapolated to the calorimeter, the acceptance depends on the photon energy. The MC simulation takes into account photon radiation in the final state [14]. The MC calculation thus provides a fully inclusive acceptance, which is 0.3% lower than that obtained with a pure $K_S \rightarrow \pi^+\pi^-$ simulation.

To take into account differences in the tracking efficiencies for data and MC, the acceptance calculation is performed by weighting the contribution of each single pion with the ratio $\epsilon_{\text{trk}}^{\text{data}}/\epsilon_{\text{trk}}^{\text{MC}}$. The single-track efficiencies ϵ_{trk} for data and MC are evaluated using $K_S \rightarrow \pi^+\pi^-$ events, as a function of transverse and longitudinal track momenta.

The MC calculation is also corrected for data-MC differences in the efficiency ϵ_{T_0} for a single pion with impact on the calorimeter to provide a T_0 cluster. This is evaluated using various data control samples as a function of the track momentum and the angle of impact on the EMC, distinguishing between π^+ and π^- tracks (or μ^+ and μ^- tracks, in case of in-flight pion decays), and separately treating tracks reaching the barrel or the endcaps.

The values of a_{cr} and $a_{\bar{cr}}$ are listed in Tab. 2, together with the number of events selected as $\pi^+\pi^-$. The errors quoted on a_{cr} and $a_{\bar{cr}}$ are due to the statistics of the MC sample and of the control samples used for the efficiency determination. The maximal variation of the acceptance during data taking is $\sim 2\%$, and is due to variations in the machine operating conditions (background levels and center of mass energy). The acceptance $a_{\bar{cr}}$ is $\sim 3\%$ lower than a_{cr} for all values of E_{cr} , because of the presence of K_L 's decaying into charged particles before reaching the EMC, which disturb the reconstruction of K_S pion tracks. The value of a_{cr} increases by 0.8×10^{-3} as the E_{cr} cut is moved from 125 to 300 MeV. This is due to a small contamination from late K_L decays in the K_{cr}^{true} sample, which is suppressed when the K_{cr} energy cut is raised. The above variation is taken as a conservative estimate of the systematic error from the simulation of this K_S - K_L disturbance. A further contribution to the systematic error comes from the T_0 efficiency correction, ϵ_{T_0} ; it is estimated to be 1.4×10^{-3} at $E_{cr}=300$ MeV (Tab. 5).

The purity of the $\pi^+\pi^-$ sample is estimated by MC to be ~ 0.9989 and is independent of E_{cr} (see Tab. 2). Two sources contribute to the background contamination: K_S decays to semileptonic final states ($\sim 0.7 \times 10^{-3}$) and $\phi \rightarrow \pi^+\pi^-\pi^0$ decays ($\sim 0.4 \times 10^{-3}$). Events of the latter type enter the selection

when an early accidental cluster induces the T_0 and one of the two high-energy photons from the π^0 is erroneously selected as K_{cr} . The systematic error on the purity comes from the uncertainty on the BR's for the decays involved and, for the $\phi \rightarrow \pi^+\pi^-\pi^0$ contribution, from the uncertainty on the rate R_{acc} . The error for these sources is evaluated to be 0.1×10^{-3} at $E_{\text{cr}} = 300 \text{ MeV}$ (Tab. 5).

E_{cr} cut	125 MeV	200 MeV	300 MeV
$N(\times 10^3)$	1218.00	907.41	490.92
a_{cr}	0.6187(5)	0.6192(6)	0.6195(8)
$a_{\overline{\text{cr}}}$	0.5968(5)	0.5991(5)	0.6016(5)
C	0.99882(4)	0.99891(4)	0.99886(6)

Table 2

Values for the observed yield, the acceptance, and the purity of the $\pi^+\pi^-$ selection, for data sample no. 10 and minimum K_{cr} energies of 125, 200, and 300 MeV. Statistical errors are shown in parentheses.

4.3 Acceptance and purity for $K_S \rightarrow \pi^0\pi^0$

The $K_S \rightarrow \pi^0\pi^0$ acceptance is evaluated from MC. To take into account data-MC differences in the cluster efficiency for low-energy photons, the acceptance calculation is performed by weighting each photon with the ratio $\epsilon_{\text{cl}}(\text{data})/\epsilon_{\text{cl}}(\text{MC})$. The single-photon detection efficiencies ϵ_{cl} for data and MC are evaluated using samples of $\phi \rightarrow \pi^+\pi^-\pi^0$ events, as a function of photon energy and polar angle.

The value of a_{cr} is listed in Tab. 3. The maximal variation for the acceptance during data taking is $\sim 1\%$ and is due to variations in the machine conditions. The various sources of systematic uncertainty on the acceptance evaluation are discussed below.

A first contribution to the systematic uncertainty on the photon counting arises from uncertainty in the data-MC cluster-efficiency correction. This has been evaluated by varying the cut on the minimum cluster energy from the default value of 20 MeV to values between 7 and 50 MeV and checking the stability of the number of selected events after efficiency corrections. The associated fractional systematic error is evaluated to be 0.5×10^{-3} . When the cut is moved from 20 to 50 MeV, the acceptance decreases by $\sim 16\%$. The data-MC cluster efficiency correction is ~ 0.9965 with the cut at 20 MeV, and negligible with the cut at 50 MeV.

Additional uncertainties in photon counting arise from data-MC differences for the probability for a photon to produce more than one prompt cluster (splitting) or convert to an e^+e^- pair before entering the DC. The corresponding

uncertainties are estimated to be 0.11×10^{-3} and 0.38×10^{-3} , respectively. The total systematic error on the acceptance due to photon counting is therefore 0.64×10^{-3} at $E_{\text{cr}} = 300 \text{ MeV}$ (Tab. 5).

A source of systematic bias is the presence of machine background clusters, which give the T_0 in 1-2% of the events (see Fig. 2 in Sec. 4.1). This causes the time of flight to be wrongly estimated, resulting in a loss of $\pi^0\pi^0$ events. The uncertainty in the method used to extract the rate of accidental clusters R_{acc} (Sec. 2) is therefore reflected in the systematic error on the acceptance. However, the $\pi^+\pi^-$ tracking efficiency is also affected because of drift times are wrongly evaluated. The two effects partially cancel when evaluating the ratio of $\pi^+\pi^-$ and $\pi^0\pi^0$ acceptances, leaving a residual systematic error of 0.52×10^{-3} at $E_{\text{cr}} = 300 \text{ MeV}$ (Tab. 5).

A further loss of $\pi^0\pi^0$ events occurs when the T_0 determination is wrong because two photons hit the same calorimeter cell, or because instrumental effects spoil the time reconstruction of a single photon (wrong T_0 from K_S). The fraction of events lost because of these mechanisms is $\sim 1\%$. The associated correction has been evaluated from data samples of $K_S \rightarrow \pi^0\pi^0$ events tagged by $K_L \rightarrow \pi^+\pi^-\pi^0$ decays in the DC, which can be selected independently of the T_0 determination. The corresponding systematic error is 0.61×10^{-3} (Tab. 5).

The number of events selected as $\pi^0\pi^0$ is shown in Tab. 3. The $\pi^0\pi^0$ sample is contaminated mainly by K^+K^- events: one of the two kaons undergoes a decay to $\pi^\pm\pi^0\pi^0$ near the origin, while the other decays to π^0 's within the DC. If the flight path of this kaon is between ~ 90 and $\sim 160 \text{ cm}$, one of the two photons from the π^0 decay can be mistagged as a K_{cr} . The purity C is evaluated from MC and depends on E_{cr} as shown in Tab. 3. A systematic error on this estimate comes from the uncertainties on the BR's involved in the decay chain and from the acceptance for decay to $\pi^\pm\pi^0\pi^0$. The uncertainty is 0.35×10^{-3} at $E_{\text{cr}} = 125 \text{ MeV}$ and negligible at $E_{\text{cr}} = 300 \text{ MeV}$ (Tab. 5). A minor source of background, also included in C , is machine background capable of satisfying the K_{cr} tag while at the same time containing three prompt clusters. The residual contamination is evaluated using data; it is 0.13×10^{-3} at $E_{\text{cr}} = 125 \text{ MeV}$ and decreases by a factor of two at $E_{\text{cr}} = 300 \text{ MeV}$. The systematic error due to these events is conservatively estimated equal to the contamination itself.

4.4 Trigger, cosmic-ray veto, and offline filter efficiencies

The trigger efficiency for both channels is obtained from data. K_L interactions always fire at least one trigger sector. About 40% of the time, however, the

E_{cr} cut	125 MeV	200 MeV	300 MeV
$N(\times 10^3)$	811.79	587.68	312.90
a_{cr}	0.8905(7)	0.8911(8)	0.8910(9)
C	0.9940(1)	0.99761(8)	0.99938(6)

Table 3

Values for the observed yield, the acceptance, and the purity of the $\pi^0\pi^0$ selection, for data sample no. 10 and minimum K_{cr} energies of 125, 200, and 300 MeV. Statistical errors are shown in parentheses.

K_{cr} fires two adjacent sectors, thus producing a valid trigger by itself. These events are used to find the probability that at least one K_S decay product complements the K_{cr} cluster to satisfy the trigger condition in the remaining 60% of the events. The trigger efficiency ϵ_{trg} as a function of E_{cr} is given in Tab. 4 for $\pi^+\pi^-$ and $\pi^0\pi^0$ events. The maximal variations of ϵ_{trg} during data taking are 0.5% and 0.1%, respectively, and are due to variations of the energy threshold of the calorimeter trigger. The systematic error is evaluated using MC events as the difference between the result of the above method and the MC truth. It is 0.25×10^{-3} for $\pi^+\pi^-$ events with $E_{\text{cr}} = 300$ MeV, and negligible for $\pi^0\pi^0$.

For $\pi^+\pi^-$ events the trigger inefficiency is $\sim 1.3\%$, as opposed to $\sim 0.1\%$ for $\pi^0\pi^0$ events. Therefore, an additional systematic error for $\pi^+\pi^-$ events arises because of the contribution of accidental clusters to the trigger. This is checked using an independent estimate of the trigger efficiency on $\pi^+\pi^-$ events, which is obtained by weighting MC kinematics with data-extracted trigger-sector efficiencies. In contrast to the method for determining the trigger efficiency described above, this method does not include the possible contribution to the trigger from accidental clusters. The difference between the results from the two methods is 0.62×10^{-3} ; this is taken as a further systematic error on the trigger efficiency.

The combined systematic error on the ratio of trigger efficiencies is estimated to be 0.67×10^{-3} at $E_{\text{cr}} = 300$ MeV (Tab. 5).

The cosmic-ray veto causes $\sim 3.5\%$ of the events selected with a K_{cr} tag to be lost. The difference between veto efficiencies for $\pi^+\pi^-$ and $\pi^0\pi^0$ is very small, since in the majority of the rejected events the K_{cr} cluster satisfies the cosmic-ray veto by depositing energy in two adjacent sectors of the outermost EMC layer, and this is independent of the K_S decay channel. However, veto efficiencies are evaluated for each channel using a subsample of selected events for which the cosmic-ray veto was recorded but not enforced at acquisition. The cosmic veto efficiency ϵ_{cv} is given in Tab. 4 for $\pi^+\pi^-$ and $\pi^0\pi^0$. The maximal variation during data taking of these efficiencies is $\sim 2 \times 10^{-3}$. The statistical error on the ratio of $\pi^+\pi^-$ and $\pi^0\pi^0$ efficiencies is $\sim 0.2 \times 10^{-3}$ and is included in the statistical error on the efficiency corrections (Tab. 5).

The inefficiency of the FILFO offline filter is estimated by MC to be smaller than 10^{-3} both for $\pi^+\pi^-$ and $\pi^0\pi^0$ events (see Tab. 4). The reliability of this prediction has been checked by studying a data subsample for which the FILFO decision is registered but not enforced during reconstruction. The systematic error on the ratio of FILFO efficiencies is estimated to be 0.74×10^{-3} at $E_{\text{cr}} = 300$ MeV (Tab. 5).

E _{cr} cut		125 MeV	200 MeV	300 MeV
$\pi^+\pi^-$	ϵ_{trg}	0.9863(1)	0.9867(1)	0.9879(2)
	ϵ_{CV}	0.9646(3)	0.9626(4)	0.9598(6)
	ϵ_{FILFO}	0.99964(2)	0.99963(3)	0.99944(4)
$\pi^0\pi^0$	ϵ_{trg}	0.99948(3)	0.99948(3)	0.99951(4)
	ϵ_{CV}	0.9625(9)	0.959(1)	0.954(2)
	ϵ_{FILFO}	0.99956(3)	0.99953(3)	0.99937(5)

Table 4

Values for the trigger, cosmic-ray veto, and FILFO efficiencies for $\pi^+\pi^-$ and $\pi^0\pi^0$ events, for data sample no. 10 and minimum K_{cr} energies of 125, 200, and 300 MeV. Statistical errors are shown in parentheses.

5 Result

The ratio $N(\pi^+\pi^-)/N(\pi^0\pi^0)$ for $E_{\text{cr}} = 300$ MeV is shown in the left panel of Fig. 3. The data have been divided into 17 samples of comparable statistical weight; the variations observed, well beyond the statistical fluctuations, are correlated to those in the overall efficiencies. The first six samples correspond to data collected during 2001, in which machine conditions were more unstable than those observed in 2002 (samples 7 to 16). The last sample refers to data from a dedicated scan performed by varying the center of mass energy by ± 3 MeV around the ϕ peak. Each measurement of R_S^π is obtained by correcting the number of $\pi^+\pi^-$ and $\pi^0\pi^0$ events for the selection efficiencies and for the background contamination (Eqs. 2 and 4). In order to avoid statistical correlations between the event counting and the efficiency corrections evaluated from data, each sample has been split into three parts on a random basis. The first of these is used for event counting, the second for the calculation of the tagging efficiency, and the third for the evaluation of the trigger efficiency.

After all of the corrections are applied, the result for R_S^π is obtained. It is shown in the right panel of Fig. 3, where the error bars represent the total statistical error. The χ^2 probability of the fit to a constant is 62%. All quantities entering into the measurement of R_S^π are listed in Tabs. 1 to 4.

The systematic errors have been evaluated for each sample separately and then

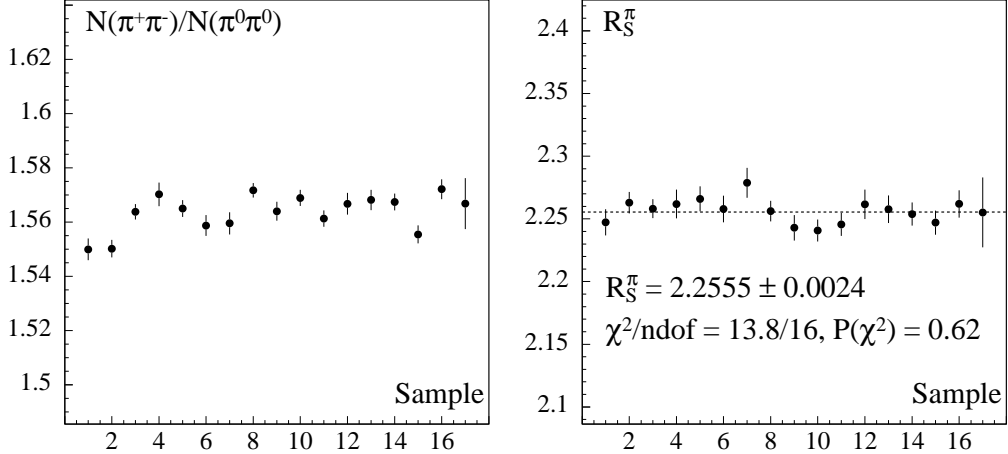


Fig. 3. Ratio $N(\pi^+\pi^-)/N(\pi^0\pi^0)$ (left panel) and result for R_S^π (right panel) for $E_{\text{cr}} = 300 \text{ MeV}$, for 17 data samples. The error bars represent the total statistical error. The result of a fit of R_S^π to a constant and the associated χ^2 are also shown.

averaged by weighting the result from each sample with the corresponding statistical error. The various contributions to the total statistical and systematic errors are shown in Tab. 5 for K_{cr} minimum energies of 125, 200, and 300 MeV.

The final result is obtained by choosing the value of E_{cr} which minimizes the total error. The best accuracy is obtained for a cut of 300 MeV (see Tab. 5). The result is:

$$R_S^\pi = 2.2555 \pm 0.0012_{\text{stat}} \pm 0.0021_{\text{syst-stat}} \pm 0.0050_{\text{syst}}, \quad (5)$$

where the first error is from the statistics of $\pi^+\pi^-$ and $\pi^0\pi^0$ events, the second is due to the statistical error in estimating all of the corrections, and the last is the systematic uncertainty.

Some of the corrections show variations as a function of E_{cr} : the most important of these are the tagging efficiencies (ϵ_{cr} and A , Tab. 1), and the contamination in the $\pi^0\pi^0$ selection (C , Tab. 3). In order to check the reliability of these corrections, the results of the analysis are compared when choosing E_{cr} values of 125, 200, and 300 MeV. Note that the event yield decreases by a factor of three going from 125 to 300 MeV. In order to avoid correlation effects in the comparison, the data set has been split using a finer granularity, corresponding to 94 samples, each of $\sim 5 \text{ pb}^{-1}$ of integrated luminosity. The analysis is performed using a different energy cut on each successive sample. The χ^2 of the three values obtained has a probability of 21% (see Tab. 6).

The present result (Eq. 5) should be compared with the result from the analysis of the year 2000 data sample [4],

$$R_S^\pi = 2.236 \pm 0.003_{\text{stat}} \pm 0.015_{\text{syst}}, \quad (6)$$

E _{cr} cut		125 MeV	200 MeV	300 MeV
Source		Fractional statistical error, (10 ⁻³)		
Event count, “stat”		0.34	0.40	0.54
Efficiencies, “syst-stat”		0.55	0.65	0.93
Total statistical		0.64	0.76	1.1
Source		Fractional systematic error, (10 ⁻³)		
$\pi^+\pi^-$	K_S - K_L disturbance	0.80	0.80	0.80
	ϵ_{T0} correction	2.0	1.8	1.4
	Background	0.10	0.10	0.10
$\pi^0\pi^0$	Cluster counting	0.76	0.58	0.64
	Wrong T_0 from K_S	0.60	0.60	0.61
	Physics background	0.35	0.14	0.04
	Machine background	0.13	0.09	0.07
$\pi^+\pi^-/\pi^0\pi^0$	Accidental rate R_{acc}	0.47	0.48	0.52
	f_n , P_n^{in} , P_n^{out} evaluation	0.67	0.53	0.45
	ϵ_{cr}	0.39	0.62	0.44
	Trigger	0.91	0.78	0.67
	FILFO	0.45	0.46	0.74
Total systematic		2.8	2.5	2.2
Total		2.8	2.6	2.5

Table 5

Contributions to the statistical and systematic uncertainties, for minimum K_{cr} energy of 125, 200, and 300 MeV.

K_{cr} energy cut (MeV)	125	200	300
R_S^π	2.2574 ± 0.0025	2.2519 ± 0.0027	2.2590 ± 0.0040
$\chi^2/\text{ndof}; P(\chi^2)$		3.12/2; 21%	

Table 6

Values of R_S^π for K_{cr} energy cuts of 125, 200, and 300 MeV, obtained from three independent samples, each with 1/3 of the entire statistics. The errors include both the “stat” and “syst-stat” contributions, as defined in the text. The χ^2 value of a fit to a constant and its probability are also shown.

where the systematic error includes also the statistical error from all of the corrections: $0.015 = 0.008_{\text{syst-stat}} \oplus 0.013_{\text{syst}}$. The error on the former result was dominated by the systematic uncertainty on the ratio of tagging efficiencies (0.011). The present analysis makes use of various improvements to the evaluation of the tagging efficiencies, as well as a larger window in β^* . This is the only relevant aspect of the analysis which has been changed with respect to that described in Ref. 4. Therefore, when combining the two results, the statistical errors and the systematic errors on the tagging efficiencies are treated as independent errors. With this assumption, the two results are com-

patible, with a probability of 18%. The two measurements can therefore be averaged. Weighting each by its independent errors and calculating the average systematic error with the same weights gives:

$$R_S^\pi = 2.2549 \pm 0.0054. \quad (7)$$

In an accompanying paper [1], this result is combined with the KLOE measurement of $\Gamma(K_S \rightarrow \pi e \nu) / \Gamma(K_S \rightarrow \pi^+ \pi^- (\gamma))$ to extract the dominant K_S BR's:

$$\begin{aligned} \text{BR}(K_S \rightarrow \pi^+ \pi^- (\gamma)) &= (69.196 \pm 0.051)\% \\ \text{BR}(K_S \rightarrow \pi^0 \pi^0) &= (30.687 \pm 0.051)\% \end{aligned} \quad (8)$$

Using their measurement of the ratio of BR's for the K_L , $R_L^\pi = 2.283 \pm 0.034$, together with the world average for $\Re(\epsilon'/\epsilon) = (1.67 \pm 0.26) \times 10^{-3}$, the KTeV collaboration quotes an expected value of R_S^π [15]: $R_S^\pi = 2.261 \pm 0.033$. This is in good agreement with the present result, Eq. 7.

Acknowledgments

We thank the DAΦNE team for their efforts in maintaining low-background running conditions and their collaboration during all data taking. We want to thank our technical staff: G. F. Fortugno for his dedicated work to ensure efficient operations of the KLOE Computing Center; M. Anelli for his continuous support to the gas system and the safety of the detector; A. Balla, M. Gatta, G. Corradi, and G. Papalino for the maintenance of the electronics; M. Santoni, G. Paoluzzi, and R. Rosellini for general support to the detector; C. Piscitelli for his help during major maintenance periods. This work was supported in part by DOE grant DE-FG-02-97ER41027; by EURODAPHNE, contract FMRX-CT98-0169; by the German Federal Ministry of Education and Research (BMBF) contract 06-KA-957; by Graduiertenkolleg 'H.E. Phys. and Part. Astrophys.' of Deutsche Forschungsgemeinschaft, Contract No. GK 742; by INTAS, contracts 96-624, 99-37.

References

[1] KLOE Collaboration, Measurement of the branching fraction and charge asymmetry for the decay $K_S \rightarrow \pi e \nu$ with the KLOE detector, submitted to Phys. Lett. B.

- [2] V. Cirigliano, J. F. Donoghue, E. Golowich, Eur. Phys. J. C18 (2000) 83, **hep-ph/0008290**.
- [3] V. Cirigliano, G. Ecker, H. Neufeld, A. Pich, Eur. Phys. J. C33 (2004) 369, **hep-ph/0310351**.
- [4] KLOE Collaboration, Phys. Lett. B538 (2002) 21.
- [5] D. E. Groom, et al., Eur. Phys. J. C15 (2000) 1.
- [6] S. Eidelman, *et al.*, Particle Data Group, Phys. Lett. B592, and 2005 partial update for edition 2006.
URL <http://pdg.lbl.gov>
- [7] N. Paver, Riazuddin, Phys. Lett. B246 (1990) 240.
- [8] N. Brown, F. E. Close, Scalar mesons and kaons in ϕ radiative decay & their implications for studies of CP violation at DAΦNE, in: L. Maiani, G. Pancheri, N. Paver (Eds.), The DAΦNE Physics Handbook, Vol. 2, 1992, p. 447.
- [9] KLOE Collaboration, Nucl. Instr. and Meth. A488 (2002) 51.
- [10] KLOE Collaboration, Nucl. Instr. and Meth. A482 (2002) 363.
- [11] KLOE Collaboration, Nucl. Instr. and Meth. A492 (2002) 134.
- [12] F. Ambrosino *et al.*, KLOE Collaboration, Nucl. Instr. and Meth. A534 (2004) 403, **physics/0404100**.
- [13] C. Gatti, M. Palutan, T. Spadaro, KLOE Note 209 (2006).
URL <http://www.lnf.infn.it/kloe/pub/knote/kn209.ps>
- [14] C. Gatti, Monte Carlo simulation for radiative kaon decays, to be published in Eur. Phys. J. C, **hep-ph/0507280**, and references therein.
- [15] KTeV Collaboration, Phys. Rev. D70 (2004) 092006, **hep-ex/0406002**.